# Coreless Fast Pulsed-Power Drivers

P.-A. Gourdain, M. Evans, P. Efthimion, R. Ellis, W. Fox, H. R. Hasson, H. Ji, R. V. Shapovalov, J. R. Young, and I. West-Abdallah

***Abstract*— Linear transformer drivers can generate mega-amperes in hundreds of nanoseconds, allowing to produce matter under extreme conditions and study it in a laboratory setting. Drivers using this technology are more compact than Marx-banks drivers but have very similar characteristics. The key component is the magnetic core that allows to charge the system in parallel, during the dc phase when the core inductance is an ignorable part of the circuit, and to discharge it in series, during the pulsed phase when the core provides inductive isolation. However, the magnetic core increases the weight, the cost of the system, and the footprint of the device. In this article, we show how the magnetic core can be replaced by an insulator break, providing capacitive isolation instead. This approach reduces both weight and footprint of the system while minimizing current losses compared with a system with cores or no isolation whatsoever.**

***Index Terms*— Linear transformer driver (LTD), pulsed power.**

## I. Introduction

LINEAR transformer drivers (LTDs) [1], [2] can become a compact replacement of Marx-driven pulsed-forming lines (PFLs). Besides their size, LTDs can be modeled using lumped circuit elements, simplifying the design and operations of the machine. The transformational technology behind LTD rests with 100-kV capacitors that can discharge 50 kA in 100 ns, whereas Marx banks used microsecond capacitors and PFL to reach similar discharge currents and rise times. These fast capacitors are connected to a spark gap switch and are typically charged up to +/−100 kV. Two capacitors connected by a spark-gap switch form a unit called a brick. In turn, the bricks are connected to a set of radial strip lines. The system is enclosed inside a metal casing, forming what is called a cavity. The strip lines connect to a set of transmission lines outside of the casing, moving efficiently the energy from the device to the target load. The casing has three functions. It keeps the electrical components together. It virtually eliminates the electromagnetic noise created by the spark gaps, acting as a Faraday cage. Finally, it contains the dielectric oil required to avoid electrical breakdown during operations. Unfortunately, the casing also acts as a perfect short circuit across the transmission lines. To regain electrical isolation, a set of magnetic cores is required, increasing dramatically the inductance of current path along the casing. It is important to note that the discharge is fast enough so that all currents discussed herein as in fact surface currents. More information about LTDs can be found in [3].

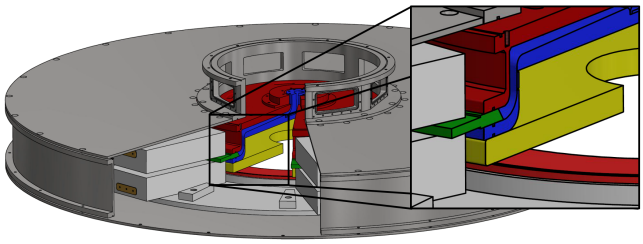

Fig. 1. Cut-out view of the coreless cavity. The outer diameter is slightly smaller than 60 in. The enlarged region shows the anode (red), the cathode (blue), and the anode–cathode insulator (green). The key component, the insulator break (yellow), separates the cathode from the bottom ground plate (light red). The casing connects electrically the anode to the ground plate. The spark-gap switches were omitted for clarity.

Impedance-matched Marx generators [4] have eliminated the need to use cores when many cavities are stacked together. Removing a portion of each casing simply eliminates the short circuit, making the cores superfluous. However, there are cases where a full casing is necessary. For instance, basic research experiments in high energy density physics can be done using one single cavity. In this case, a full casing should be used, and a short circuit would appear if cores were removed. In many applications, designers turn to capacitive isolation when inductive isolation cannot be used. This approach is especially attractive for MA-class machines [5]–[7]. By removing the magnetic cores, we can de facto reduce maintenance, footprint, cost and simplify experimental operation. There is another advantage in removing cores. It is now possible to bring the bricks closer to the transmission lines and decrease the internal inductance of the driver.

In this article, we focus on the design and numerical simulations of a mid-scale driver with no magnetic cores, capable of driving 400 kA into a matched 10-nH load in 150 ns. The proposed design is shown in Fig. 1. The inductance of the load

Manuscript received December 13, 2020; revised April 29, 2021; accepted May 26, 2021. Date of publication June 22, 2021; date of current version July 22, 2021. This work was supported in part by the NSF/DOE Partnership in Basic Plasma Science and Engineering via a DOE Office of Science, Fusion Energy Sciences Award under Grant DE-SC0016252, in part by the Princeton Plasma Physics Laboratory (PPPL) DOE Contract under Grant DE-AC02-09CH11466, in part by the NSF Major Research Instrumentation (MRI) Award under Grant PHY-1725178, in part by the NSF CAREER Award under Grant PHY-1943939, and in part by the University of Rochester. The review of this article was arranged by Senior Editor R. P. Joshi. *(Corresponding author: P.-A. Gourdain.)*

P.-A. Gourdain, M. Evans, H. R. Hasson, J. R. Young, and I. West-Abdallah are with the Department of Physics and Astronomy and the Laboratory for Laser Energetics, University of Rochester, Rochester, NY 14627 USA (e-mail: gourdain@pas.rochester.edu).

P. Efthimion, R. Ellis, W. Fox, and H. Ji are with the Princeton Plasma Physics Laboratory, Princeton University, Princeton, NJ 08543 USA.

R. V. Shapovalov is with the Department of Nuclear and Radiological Sciences, University of Michigan, Ann Arbor, MI 48103 USA.

Color versions of one or more figures in this article are available at https://doi.org/10.1109/TPS.2021.3086322.

Digital Object Identifier 10.1109/TPS.2021.3086322

is relatively small to allow capacitors with a charged voltage limited to +/−100 kV to deliver 400 kA to drive compact loads, such as radial foils [8] or hybrid x-pinches [9]. At the location where the cores have been removed, the transmission lines are separated by two insulators. The first insulator (green in Fig. 1) separates the anode from the cathode (red and blue, respectively, in Fig. 1). This insulator is found in all LTD designs. The second insulator (yellow in Fig. 1) separates the cathode from the ground plate (shown in light red Fig. 1). The ground plate is electrically connected to the anode via the casing. This insulator is the innovative part of the proposed system.

To evaluate the performance of this pulsed-power driver, we modeled the transmission lines using a fully electromagnetic, time-dependent model. We used finite elements to track the time evolution of an electromagnetic wave traveling from the capacitors to the load, located at the center of the radial transmission lines, while measuring the currents in both driver and load. The capacitors, load, and the spark gap switches inside the casing were modeled as lumped components. However, the rest of the system was discretized using finite elements to provide an accurate description of the current evolution throughout the discharge into a matched load. The problem was solved using COMSOL, as described in [10]. We also modeled the transmission lines using lumped elements to compare electromagnetic simulations with circuit simulations done using SPICE. Section II describes the design and modeling strategy used in this article. We then present the results of our simulations.

## II. Design and Modeling

### A. System Design

The cavity uses a clamshell design to compress all the vacuum facing components together, an approach successfully implemented on HADES [11] and relatively robust when the cavity lies horizontally. The clamping force relies on the height difference between the central stack and the outer ring. When the lids are tight shut, they compress the o-rings across the central stack, making an excellent vacuum seal. The force can be computed analytically [12] and the height difference between the inner ring stack and the outer ring is directly related to the clamping force. The design is shown in Fig. 1. The anode (red in Fig. 1) is designed to take the clamping force and distribute it evenly to seal the o-ring against the rexolite anode–cathode insulator (green in Fig. 1). The clamping force also pushes against the ground plate (light red in Fig. 1) and the force is carried to the cathode (blue in Fig. 1) that also seals against the anode–cathode insulator. Finally, the insulator plate (yellow in Fig. 1 and referred to as the insulator in the rest of this article) closes the gap between the anode and the ground plate. The insulator break extends radially inward two inches above the vacuum port and protects the turbo pump from debris falling from the vacuum chamber above.

Removing the cores and replacing them with an insulator have several advantages. It brings the capacitors closer to the load, reducing the overall inductance of the driver as well as its footprint. It helps with maintenance, limiting the amount of trapped air bubbles inside the oil. It also simplifies daily operations as premagnetization is not required. The insulator break thickness was picked based on mechanical stiffness, rather than dielectric strength, limiting the deformations caused by compression, both from the clamshell and vacuum.

### B. Cavity Modeling

We approached our modeling in three different ways. First, we assumed that the cavity could be modeled using a minimal number of lumped elements. This approach implies that all the energy stored inside the capacitors flows through one single path leading to the target load via the transmission lines, shown in Fig. 1 (colored blue and red), modeled as a perfect inductor. In the second approach, we used 2-D electromagnetic simulations. We assumed that the system was perfectly axi-symmetric. We only removed the bricks from the simulation domain, keeping all the other components (e.g., insulators, transmission lines, casing). We coupled the simulation domain to a lumped circuit representing the bricks instead. The load was also coupled to the computational domain in the same manner. In the final approach, we only modeled the transmission lines in 3-D. A smaller domain allowed for a substantial reduction in computation time. As in the first approach, we assumed that all the energy inside the capacitors was transferred to the load. These simulations were used to optimize the gap between the transmission lines while considering the vacuum vents crossing the anode and the cathode, breaking the symmetry of the system. As a result, only 1/12th of the geometry was modeled, using boundary conditions, accounting for the six planes of symmetry. If at any point in the simulation the electric field across the transmission lines reached the emission field (taken to be 200 kV/cm for stainless steel), we could expect arcing to take place. So, the gap between the cathode and anode was increased until the electric field went below the emission value everywhere along the transmission line surface. In all three cases, we let the simulations evolve in time during half a cycle, until the current passes its peak. We stopped all simulations after 300 ns. In all cases, we used +/−95 kV as the initial capacitor charge.

The mechanical design presented in Fig. 1 was turned into an equivalent circuit using lumped elements. The transformation is relatively straightforward. First, the bricks are all distributed homogeneously around the circumference of the machine, allowing to suppose the system axisymmetric. In Fig. 2(a), we represented the centerline of the device as a vertical dot-dashed line. The casing shape is represented by the gray open square surrounding the bricks.

While not necessary, we kept the circuit symmetric, highlighting the brick structure in Fig. 2(a). In our model, the capacitors have a parasitic resistance $R_C$, a parasitic inductance $L_C$, and a capacitance $C$. Each capacitor in the simulation has a capacitance of $C = 12 \times 60$ nF, since the pulser has 12 bricks in parallel. We used values provided by the manufacturer for the residual resistance of $R_C = 0.1/12\ \Omega$ and inductance $L_C = 50/12$ nH for our 12 bricks connected in parallel. We also grouped all switches together. They were approximated as an inductor $L_S$ and a resistor

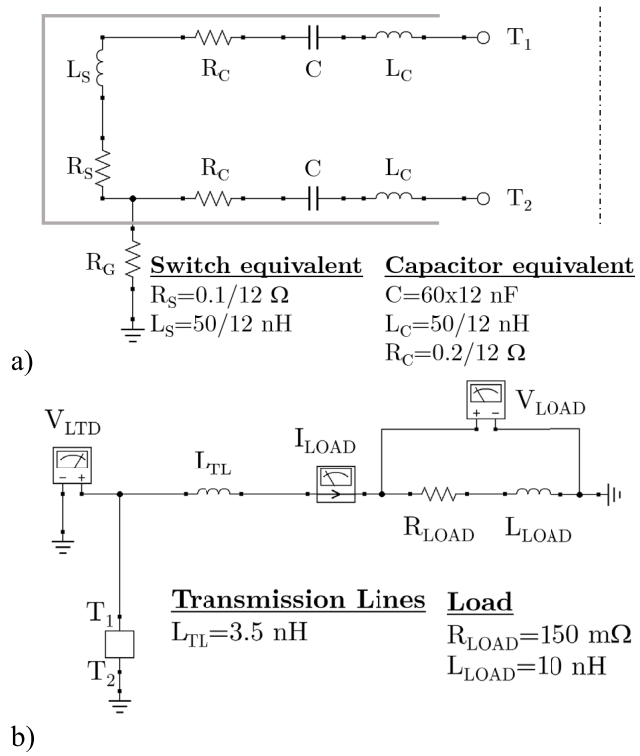


Fig. 2. (a) Equivalent *RLC* circuit for one coreless cavity with 12 bricks used in SPICE simulations. $T_1$ and $T_2$ are the terminals used to connect the cavity to the radial transmission lines and the load. The $R_G$ is a resistor 5 MΩ used to stabilize computations. (b) Equivalent *RLC* circuit for the whole system. The block with terminals $T_1$ and $T_2$ uses the subcircuit shown in (a).

$R_S$. The circuit is connected to a set of transmission lines via the connection point $T_1$ and $T_2$ [shown in Fig. 2(b)]. The transmission line inductance $L_{TL}$ was computed precisely from CAD drawings. The load is a simple $R-L$ circuit. The resistor value is chosen to match the characteristic impedance of the system $Z = \text{sqrt}(L/C)$ where $L$ and $C$ are the inductance and capacitance values of the overall equivalent system. The location of the voltmeters and ammeters used to measure the electrical response of the circuit is also indicated.

While this approach characterizes well the current rise time and its peak value, it also has some drawbacks. Modeling transmission lines more accurately require a large set of lumped elements using a T- or Π-based ladder network to account for the unique geometry of the radial transmission lines with variable anode cathode gap. Furthermore, the gap was not initially optimized to keep the electric field below the emission value and using this approach to minimize the gap could be cumbersome compared to modern techniques, which link CAD models to full electromagnetic simulations seamlessly.

We used the implicit electromagnetic solver of COMSOL to minimize the gap and compute the current waveform at the same time. The equivalent circuit of the 12 bricks is presented in Fig. 2, also showing the location of the ammeter and voltmeter. The voltmeter measures the voltage across the load and the ammeter records the current flowing inside the load. While switch closure is instantaneous in the lumped

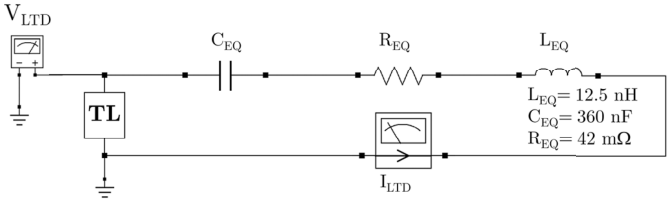


Fig. 3. Equivalent *RLC* circuit for the coreless cavity used in 2-D COMSOL simulations. TL indicates the connection to the transmission lines modeled in COMSOL.

circuit model, the spark-gap closing time must be smooth to keep relatively large time steps in the full electromagnetic simulations. We used a variable inductance $L_t$ following the time evolution given as follows:

$$L_t = \frac{1}{2} L_{\text{START}} \left[ 1 - \tanh\left( \frac{t}{t_{\text{rise}}} \right) \right] + L_{\text{EQ}}$$

where $L_{\text{START}} = 1\ \mu\text{H}$, $L_{\text{EQ}} = 12.5$ nH, and $t_{\text{rise}} = 5$ ns. This approach limits numerical instabilities inside the simulation. This technique was found more effective than using a time varying resistor [10]. Starting with high resistance reduced dramatically the initial time steps of the simulation caused by stiff equations. Even a Smooth turn-on can have transient reflections. Another important aspect of the electromagnetic simulations is to realize that real pulsed-power transmission lines are in fact slightly lossy. This is caused in part by series resistive losses in the conductors and in part by the perpetual outgassing of the transmission line surface and leads to shunt resistive losses. While current losses should be minimized, small resistive losses have a big advantage numerically; they virtually eliminate reflections caused by transients in lossless transmission lines. We have found that a small vacuum conductivity (∼0.1 mS/m) is enough to eliminate most transients at system turn-on.

There is a tradeoff since the lumped circuit simulations are relatively fast compared with the electromagnetic simulations. However, the gap optimization can be done relatively quickly using the fact that the cavity is quasi-axisymmetric. The 2-D simulations are still much longer than lumped circuit simulations. Yet, the simulation time is still short enough to beat lumped circuit simulations when the transmission line geometry is changed in between simulations. It takes less than four minutes to do an electromagnetic simulation on a laptop computer (using one processing core). The strong scaling of the electromagnetic simulations allows to divide this time by $N$ if we used $N$ CPU cores.

We also used 3-D simulations to verify that any nonaxisymmetric alterations of the transmission lines did not enhance the electric field locally. One example was the vacuum vents cut inside the lines to allow air to flow more freely inside the chamber when pumps are located only below the cavity. Without vents, air would have to be pumped from above and below the cavity. We reduced the domain substantially to reduce the computation time. First, we modeled only 1/12th of the geometry, considering multiple planes of symmetry. Second, we coupled the circuit of Fig. 2(a) directly to the entrance of the transmission lines, at the location of the

anode–cathode insulator, supposing that the current only flows through the transmission lines. If we suppose that the whole current flows through the transmission lines, we will obtain the maximum possible electric field across the anode–cathode gap. The 3-D simulations took ten minutes to run on a 40-core workstation.

## III. Numerical Simulations

### A. Overall Results

The lumped circuit approach gives a good approximation of the current peak and rise time for a 10-nH load with a 0.15-Ω matched resistor. While it is possible to refine the circuit model further to get a better estimate, we have found that modeling the transmission lines as a simple inductor is acceptable for an initial design. The simulation gives a maximum current of 421 kA at 124 ns. The overall time evolution of the current is shown in Fig. 4(a). At peak current, all inductive voltages disappear, and the power supply voltage is simply the load resistive voltage, on the order of 64 kV. For this load, we can compute the instantaneous real power (as opposed to reactive power) of the device, slightly below 27 GW.

It is interesting to compare this model with a more precise simulation using the full electromagnetic solver. While we have assumed that all the energy is coupled into the load in the first approach, the electromagnetic simulation accounts for the delocalization of all lumped elements, which are truly distributed across the whole system. Fig. 4(b) shows the current flowing inside the driving circuit (ammeter labeled $I_{\mathrm{LTD}}$ from Fig. 3) and the current flowing through the load ($I_{\mathrm{LOAD}}$, measured in the load circuit and not shown here) are the same. The current rises to 444 kA in 153 ns. We can see that both simulations give consistent results, despite the simplified lumped element approximation, which slightly underestimates the current rise time and peak current [10]. We see a slight difference at the beginning of the discharge, due to displacement currents across the insulator break, caused by the initially large $\mathrm{d}V/\mathrm{d}t$ [13].

We see that capacitive isolation is much more effective at minimizing parasitic current losses inside the casing than inductive isolation, using magnetic cores and shown in Fig. 4(c). This conclusion should not be generalized too quickly since the proposed design was optimized for capacitive isolation rather than inductive isolation. Moving the capacitors closer to the load has reduced the length of the radial strip lines, de facto limiting the coupling between the cores and the driving circuit. Fig. 4(c) shows that the losses are rather severe for this nonoptimized case. The peak current is well below the peak computed in the previous case, reaching 380 kA in 141 ns. Because the inductive isolation is less effective, the overall impedance seen by the driving circuit is lower, reducing substantially the driving voltage. It is interesting to compare this result with the case where no isolation is used, plotted in Fig. 4(d). The current peaks at 308 kA in 122 ns, demonstrating that, it is better to have inductive isolation rather than no electrical isolation whatsoever.

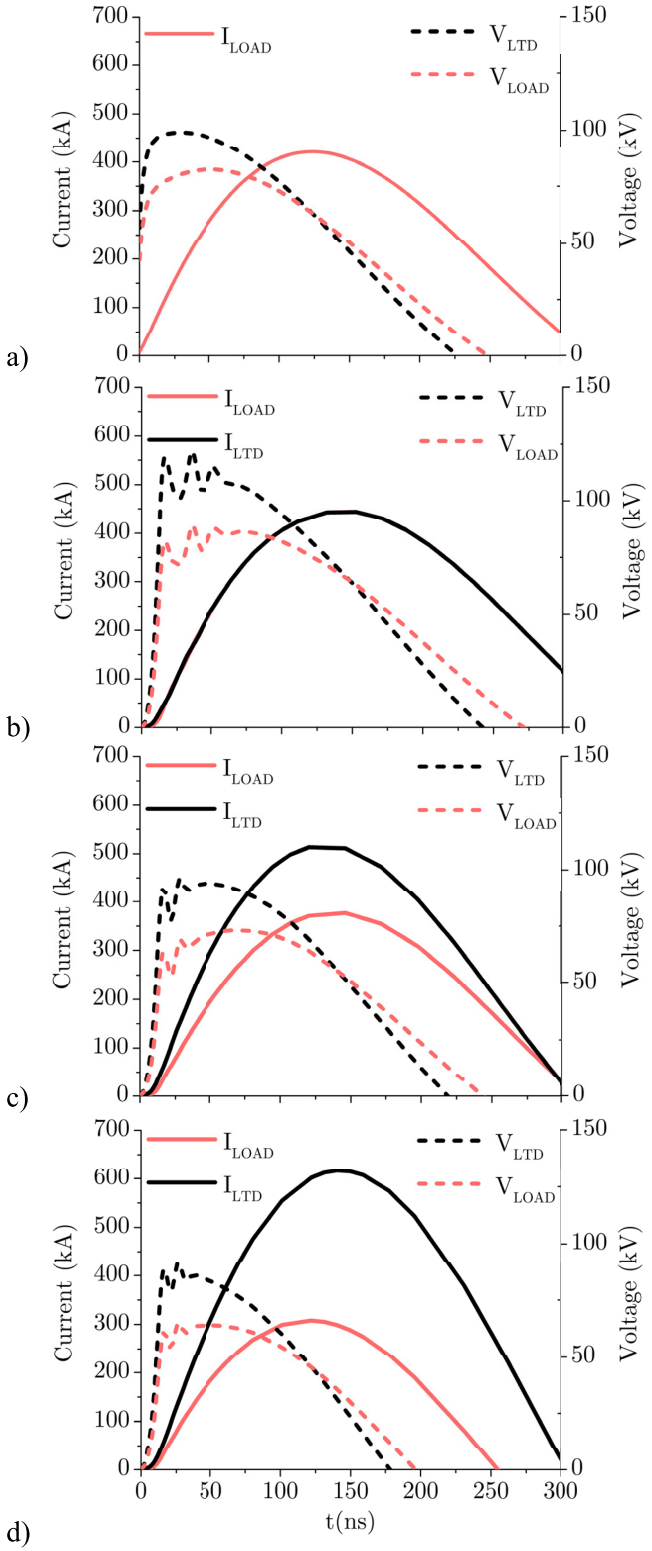


Fig. 4. (a) Lumped circuit model based on the circuit presented in Fig. 2(a) and (b). Since the presence of the casing is ignored, we do not plot the current flowing through the capacitors. Full electromagnetic simulations using the circuit presented in Fig. 3 as the drive using (b) insulator, (c) set of cores, and (d) neither.

### B. Transmission Line Optimization

The previous section shows simulation with optimized transmission lines, where the anode–cathode gap was reduced

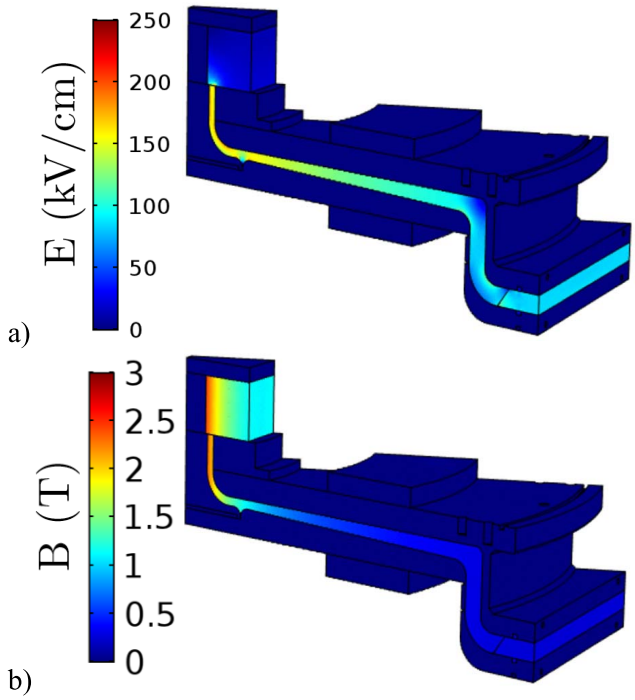


Fig. 5. Maximum (a) electric and (b) magnetic fields across the transmission lines.

as much as possible. However, electromagnetic simulations were necessary to arrive to this result. They were done in two steps. First, we used 2-D electromagnetic modeling to define an acceptable anode–cathode gap. Then, the inductance of the transmission line was computed from the technical drawings and used in the lumped component simulation to check electromagnetic simulations.

The gap was kept constant from the anode–cathode insulator all the way to the end of the vertical section of both transmission lines. It is much easier to manufacture pipes than conical tubes. Circular tubes can be welded to flat plates, yielding the transmission line design shown in Fig. 1. It is relatively more difficult to produce conical shapes, especially for bigger parts. Since the same set of transmission lines were used in all of the electromagnetic simulations discussed in Section III-A, the conclusions remain the same regardless of the transmission line shape.

Our final design is presented in Fig. 5. A practical consideration required 3-D modeling, due to the break in the axisymmetry caused by vacuum slots. Despite these slots, Fig. 5(a) shows that the maximum electric field is below the emission field throughout the anode–cathode gap. We also plotted the magnetic field distribution at maximum current, reaching of 2.25 T in the load region, as shown in Fig. 5(b).

## IV. Conclusion

This article showed that an LTD design can be slightly altered by replacing inductive isolation with capacitive isolation. The design is straightforward and simply replaces the magnetic cores with an insulator break, which isolates the cathode from the grounded cavity. While it might be possible to extend this approach to multiple cavities connected in series or in parallel, the engineering changes for a single cavity are relatively straightforward. The cathode is the only component that should be modified to fit the insulator break. On new systems, this approach reduces stray inductance and lowers the total machine cost and its weight. For the proposed design, the insulator break performs better than magnetic cores. However, the design was not optimized for magnetic cores and we should not draw conclusion about the efficacy of either methods. Rather, this article should spawn new studies to see whether the existing systems can benefit from the approach described herein.

## References

[1] A. A. Kim *et al.*, "Development and tests of fast 1-MA linear transformer driver stages," *Phys. Rev. Special Topics Accel. Beams*, vol. 12, no. 5, May 2009, Art. no. 050402.

[2] M. G. Mazarakis *et al.*, "High current, 0.5-MA, fast, 100-ns, linear transformer driver experiments," *Phys. Rev. Special Topics Accel. Beams*, vol. 12, no. 5, May 2009, Art. no. 050401.

[3] R. D. McBride, "A primer on pulsed power and linear transformer drivers for high energy density physics applications," *IEEE Trans. Plasma Sci.*, vol. 46, no. 11, pp. 3928–3967, Nov. 2018.

[4] W. A. Stygar *et al.*, "Impedance-matched Marx generators," *Phys. Rev. A, Gen. Phys. Beams*, vol. 20, no. 4, Apr. 2017, Art. no. 040402.

[5] S. C. Bott *et al.*, "250 kA compact linear transformer driver for wire array *z*-pinch loads," *Phys. Rev. Special Topics Accel. Beams*, vol. 14, no. 5, May 2011, Art. no. 050401.

[6] R. M. Gilgenbach, M. R. Gomez, J. C. Zier, W. W. Tang, and D. M. French, "MAIZE: A 1 MA LTD-driven Z-pinch at the University of Michigan," *AIP Conf. Proc.*, vol. 1088, p. 259, Jan. 2009.

[7] F. Conti *et al.*, "MA-class linear transformer driver for Z-pinch research," *Phys. Rev. Accel. Beams*, vol. 23, Sep. 2020, Art. no. 090401.

[8] P.-A. Gourdain *et al.*, "Initial experiments using radial foils on the cornell beam research accelerator pulsed power generator," *Phys. Plasmas*, vol. 17, no. 1, Jan. 2010, Art. no. 012706.

[9] T. A. Shelkovenko *et al.*, "Dynamics of hybrid X-pinches," *Plasma Phys. Rep.*, vol. 41, pp. 52–70, Jan. 2015.

[10] P.-A. Gourdain *et al.*, "Current adding transmission lines for compact MA-class linear transformer drivers," *Phys. Rev. Accel.*, vol. 23, no. 3, Mar. 2020, Art. no. 030401.

[11] P.-A. Gourdain, M. Evans, B. Foy, D. Mager, R. McBride, and R. Spielman, "HADES: A high amperage driver for extreme states," 2017, *arXiv:1705.04411*. [Online]. Available: http://arxiv.org/abs/1705.04411

[12] W. C. Young and R. G. Budynas, *Roark's Formula for Stress and Strain*, 7th ed. New York, NY, USA: McGraw-Hill, 2002, p. 487.

[13] R. D. McBride *et al.*, "Displacement current phenomena in the magnetically insulated transmission lines of the refurbished Z accelerator," *Phys. Rev. ST Accel. Beams*, vol. 13, Dec. 2010, Art. no. 120401.